This is an *Accepted Manuscript*, which has been through the Royal Society of Chemistry peer review process and has been accepted for publication.

*Accepted Manuscripts* are published online shortly after acceptance, before technical editing, formatting and proof reading. Using this free service, authors can make their results available to the community, in citable form, before we publish the edited article. We will replace this *Accepted Manuscript* with the edited and formatted *Advance Article* as soon as it is available.

You can find more information about *Accepted Manuscripts* in the **Information for Authors**.

Please note that technical editing may introduce minor changes to the text and/or graphics, which may alter content. The journal's standard **Terms & Conditions** and the **Ethical guidelines** still apply. In no event shall the Royal Society of Chemistry be held responsible for any errors or omissions in this *Accepted Manuscript* or any consequences arising from the use of any information it contains.

# Journal Name

## ARTICLE TYPE

# Twist grain boundary (TGB) states of chiral liquid crystalline bent-core mesogens

**Hale Ocak[a,b]\*, Belkız Bilgin-Eran[b], Dilek Güzeller[b], Marko Prehm[a] and Carsten Tschierske[a]\***

**4-Cyanoresorcinol derived bent-core molecules with a chiral (*S*)-2-methylbutoxy chain form liquid crystalline phases with TGBA- and TGBC-like structures at the transition from cybotactic nematic via SmA to SmC phases.**

10 Chirality has huge effects on molecular self assembly.[1] Soft matter, especially liquid crystalline (LC) phases[2,3] can easily be affected by chirality leading to helical superstructures.[4] Molecules with high helical twisting power‡ can even give rise to the frustration of the fundamental structures of LC self-assembly,
15 thus providing new superstructures with a higher level of complexity[3] and new emerging properties. Examples are the three-dimensional lattices of defects in the blue phases which are of importance as photonic band gap materials and represent candidates for new generations of extremely fast switching
20 electro-optical devices,[5] twist grain boundary (TGB) phases,[6] representing analogues of the Arbrikosov flux phase of type-II superconductors[7] and several other complex structures.[5,8]
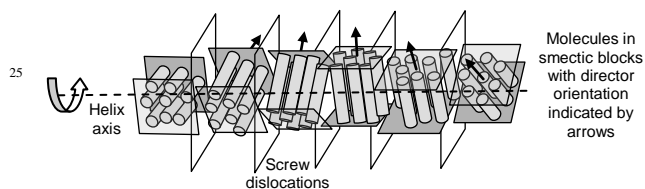


25

30 **Figure 1** Schematic image of the twist grain boundary (TGB) structure.

TGB phases, formed by chiral rod-like mesogens, represent helical superstructures with a helix axis parallel to the layer planes thus disrupting the layers into blocks separated by screw
35 dislocations (Fig. 1). TGB phases can be divided into TGBA phases with an orthogonal organization of the molecules with respect to the planes of these blocks and several different modes of TGBC phases with a tilted organization of the molecules.[6] In the recent two decades bent-core (BC) molecules[9] attracted
40 special attention as new LC materials. This is mainly due to their capability to form LC phases with polar order[9] and the spontaneous formation of chiral superstructures though the molecules are achiral.[9,10,11,12] An interesting point concerns the interaction of these chiral superstructures with the molecular
45 chirality provided by stereogenic units. For example, enhancement of chirality was observed by doping chiral LC phases with achiral bent-core mesogens, which lead to the induction of highly frustrated blue phases with helical

organization in all three directions instead of only one in the
50 cholesteric phases.[5] It was proposed, that "highly chiral" conformations[11,13] of the bent aromatic cores lead to a high twisting power.‡ For the same reason broad regions of blue phases were recently found for optically active BCLCs.[14]

55 
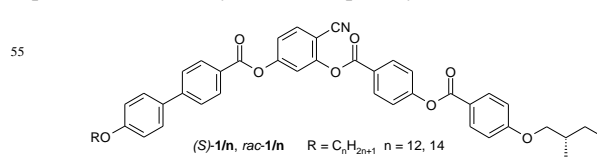
60 Herein we report the first observation of TGB-like structures for the LC phases of the BC mesogens (*S*)-**1/*n*** (*n* = 12, 14) involving a 4-cyanoresorcinol derived BC,[14b,15] combined with a chiral (*S*)-2-methylbutoxy group. In order to identify the specific chirality effects, one of the compounds was also synthesized in
65 racemic form (*rac*-**1/12**). The synthetic strategy to these BC compounds is outlined in Scheme 1 and the experimental procedures are described in the ESI.†

70 

75

80
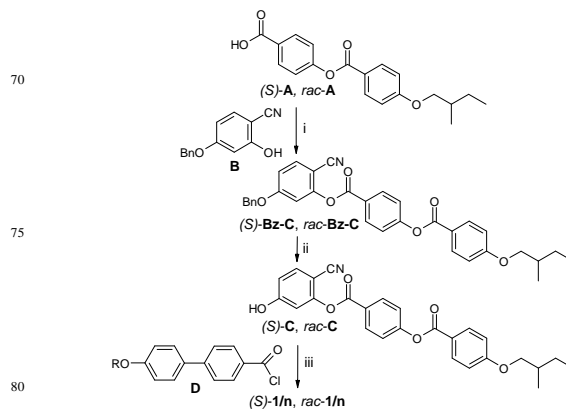
**Scheme 1** Synthesis of **1/*n***. *Reagents and conditions*: (*i*) DCC, DMAP, CH₂Cl₂, 20 °C; (*ii*) H₂, Pd/C, THF, 40 °C; (*iii*) pyridine, CH₂Cl₂, 20 °C.†

85 The observed LC phases, their transition temperatures and associated enthalpies are collated in Table 1. On cooling the racemic mixture *rac*-**1/12** from the isotropic liquid (Iso) a nematic phase (N) is formed at first which is then replaced by a lamellar phase (SmA) at *T* ≤ 96 °C. In the SmA phase there is an
90 on average non-tilted organization of the molecules in layers, whereas at the transition to the SmC phase at *T* = 88 °C a uniform tilt develops. This phase sequence was identified by the typical textures observed under the polarizing microscope (see Fig. S1†)

and confirmed by XRD (see below). In calorimetric investigations besides the dominating melting peak only the Iso-N transition could be observed by a small DSC peak (~1.1 kJ mol^{-1}), whereas there is no measurable enthalpy change for the other LC phase transitions (Fig. S7†). This indicates that major structural transformations take place at the Iso-N transition and this is in line with a cybotactic structure of the nematic phase, as confirmed by XRD (N$_{cybA}$, see below).[15b] It appears that the following phase transitions are continuous and mainly associated with the growth of the cybotactic clusters. Though the melting points are around 95-99 °C all samples can be cooled to about 60 °C without crystallization, so that also the monotropic LC phases can easily be investigated (see Table 1).

**Table 1**. Transitions of the investigated compounds [a]

| Comp. | $T/°C$  [$\Delta H$/kJ mol^{-1}] |
|---|---|
| *rac*-**1/12** | Cr 95 [34.7] (SmC 88 [<0.01]) SmA 96 [<0.01] N$_{cybA}$ 108 [1.1] Iso |
| *(S)*-**1/12** | Cr 98 [39.3] (SmC*/TGBC 88 [<0.01] TGBA 96 [<0.01]) N*$_{cybA}$ 108 [1.2] Iso |
| *(S)*-**1/14** | Cr 99 [44.9] (SmC*/TGBC 94 [<0.01]) TGBA 102 [<0.01] N*$_{cybA}$ 109 [1.4] Iso |

[a] Transition temperatures and enthalpy values (square brackets) determined by DSC (1st heating and cooling, rates 10 K min^{-1}, peak temperatures) or by PM for transitions without visible $\Delta H$; round brackets indicate monotropic (metastable) phases; abbreviations: Cr = crystalline solid; Iso = isotropic liquid; N$_{cybA}$ = cybotactic nematic phase composed of SmA clusters; N*$_{cybA}$, SmC* = chiral N$_{cybA}$ and SmC phases, respectively; SmA = non-tilted smectic phase; SmC = synclinic tilted smectic phase; TGB = twisted states of the SmA (TGBA) or SmC phases (TGBC) with helix axis parallel to the layers; for DSCs see Fig. S7.†

The phase transition temperatures of the *(S)*-enantiomer *(S)*-**1/12** are the same as found for *rac*-**1/12**. For *(S)*-**1/14** a very similar behaviour as for *(S)*-**1/12** is observed, only the transitions between the LC phases occur at a bit higher temperatures (Table 1). The typical textures observed for the LC phases of *(S)*-**1/n** (*n* = 12, 14) are shown in Fig. 2. A cholesteric oily-streak texture indicates the presence of a helical superstructure in the chiral nematic phases (N*) (Fig. 2a).[5] The appearance of the LC phases occurring below N* strongly depends on the alignment conditions. Homeotropic anchoring (layers parallel to the surfaces of the glass substrates) leads to filament textures, as characteristic for TGBA phases[16] (Fig. 2b). The filaments rapidly disappear and the textures become uniformly dark, indicating the transition to an optically uniaxial SmA phase. On further cooling, a gray and low birefringent texture develops in these homeotropic samples, indicating a transition to a SmC* phase, occurring for *(S)*-**1/12** at about the same temperature as observed for the SmA-SmC transition of the racemate.§ In a cell with planar surface anchoring (layers perpendicular to the substrate surfaces; polyimide-coated ITO cell, 10 μm) the cholesteric oily streaks texture changes at the N*-SmA transition to a planar texture composed of differently coloured areas, corresponding to different twist states (Fig. 2c). This texture, which is typical for TGBA phases, is retained on further cooling (see Fig. S2†) and at the SmA/SmC phase transition temperature the formation of a grid-like pattern is observed (Fig. 2d), similar to textures of TGBC phases.[4,6,17] The texture continuously changes on further cooling (see Fig. S3†). Therefore it is not clear if the TGBC structure is retained or a slow transition to a SmC*-phase takes

place on further cooling (therefore assigned as SmC*/TGBC in Tab. 1). As for *rac*-**1/12**, in DSC investigations no measurable transition enthalpies can be found for *(S)*-**1/12** and *(S)*-**1/14** below the Iso-N* transition until crystallization (Fig. S7†).
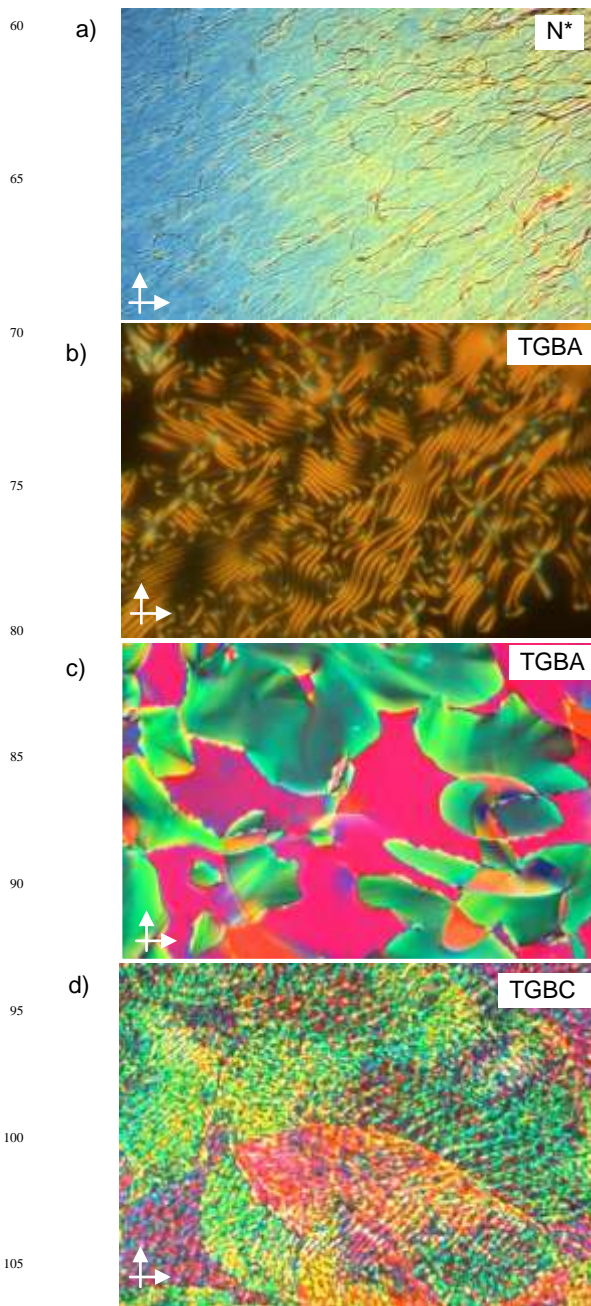
**Figure 2** Textures of the LC phases of compounds *(S)*-**1/n** between crossed polarisers: (a) oily-streak texture of the N* phase of *(S)*-**1/14** at $T$ = 107 °C; (b) fingerprint texture of *(S)*-**1/14** in the TGBA-state in homeotropic anchoring at $T$ = 96 °C (c) TGBA-state of *(S)*-**1/12** in planar anchoring (polyimide coated ITO-cell, 10 μm) at $T$ = 92 °C and d) TGBC-like texture at $T$ = 79 °C; for additional textures see Figs. S2-S5.†

XRD investigations were performed for *(S)*-**1/12** and *rac*-**1/12** in thin capillaries in a magnetic field of $B$ ~ 1 T after slow cooling (0.1 K min^{-1}) from the isotropic liquid. In the whole investigated temperature range between 60 and 110 °C the wide angle scattering is diffuse indicating the presence of LC phases

without long range order between individual molecules (Fig. 3a,b). In the small angle range there is a diffuse scattering already in the Iso phase, indicating a cybotactic structure of the isotropic liquid (Iso$_{cyb}$). The diffuse scattering is retained and grows in

5 intensity in the N and N* phases, exceeding the wide angle scattering and thus confirming cybotactic nematic phases composed of smectic clusters.[15b]
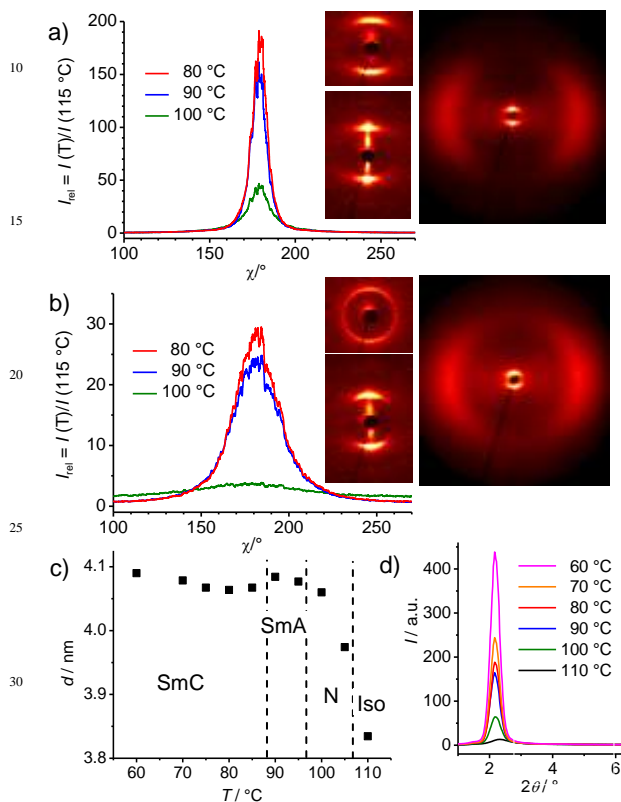






35 **Figure 3** XRD data (a,c.d) of *rac*-**1/12** and (b) of (*S*)-**1/12**. a,b) $\chi$-scans over the small angle scattering depending on *T* and corresponding 2D XRD patterns of magnetically aligned samples in the N/N* phase at *T* = 105 °C (top left) and in the tilted smectic phases (bottom and right) at *T* = 80 °C; c) *T*-dependence of the *d*-spacing and d) 2$\theta$-scan over the small 40 angle scattering depending on *T*, see Tables S1, S2 and Figs. S.9, S10.†.

For *rac*-**1/12** the small angle scattering maximum is on the meridian, indicating that the molecules have no uniform tilted in these domains, i.e. the nematic phases are composed of SmA 45 clusters (N$_{cybA}$), which is rarely found for BC molecules.[15b] The intensity of the small angle scattering increases further at the transition to the SmA phase (Fig. 3d). A weak second order reflection develops at the next phase transition to the SmC phase. The *d*-spacing of 4.05 - 4.10 nm, corresponding to ~0.85 50 molecular length ($L_{mol}$ = 4.8 nm in the most stretched conformation, see Fig. S8†), is in line with a single layer structure of the cybotactic clusters and layers. The *d* = *f*(*T*) plot for *rac*-**1/12** indicates an increase of *d* in the N and SmA phases due to an increasing packing density, leading to alkyl chain stretching. A 55 slight decrease of *d* starts around the SmA-SmC transition, in line with the onset of uniform tilt at this transition (Fig. 3c). The tilt in the SmC phase is very small (<5°) as estimated for *rac*-**1/12** from the angle between the diffuse wide angle scattering maxima on the equator and the layer reflections on the meridian (XRD tilt). 60 The optical tilt is about 10-15° as estimated from the planar

textures of *rac*-**12** (see Fig. S1g,h†), indicating that main contribution comes from the tilt of the aromatic cores.

The LC phases of (*S*)-**1/12** (Fig. 3b) have approximately the same *d*-values as *rac*-**1/12**. However, in the N* phase the small- 65 and wide-angle scatterings form closed rings, indicating the absence of uniform alignment due to the presence of the helical superstructure. At the transition to TGBA the rings condense to crescent like maxima on the meridian (small angle) and on the equator (wide angle), respectively, in line with the formation of 70 layers. There is a broader angular $\chi$-distribution of the scattering in the smectic phases of (*S*)-**1/12** compared to the sharper peak of *rac*-**1/12** (Fig. 3a,b). However, there is no distribution of the scatterings on a closed ring as it would be expected for TGB phases. So, there seems to be a strong effect of the conditions on 75 the actually observed phase structure. As shown above, planar anchoring stabilizes the TGB helix, whereas homeotropic anchoring has the opposite effect; it stabilizes the layers and tends to remove the TGB helix. Hence, the TGB structures are not considered as "phases", but as helically deformed states of the 80 underlying smectic phases. The reduced influence of surface anchoring in the capillaries used for XRD, and the alignment of the molecules by the magnetic field, might suppress TGB-helix formation. The broader angular distribution of the scattering of (*S*)-**1/12** might be due to a remaining helical layer distortion or to 85 the less efficient alignment obtained by cooling from the N* phase.

There is no polarization current response under a triangular wave field (PI coated ITO cells 10 μm) in the temperature range of all mesophases for the racemic mixtures as well as for the *(S)*- 90 enantiomers up to the maximum available value of ±28 Vμm$^{-1}$, indicating the absence of polar order. ¶

As an additional interesting point, it should be noted that chiral domains are visible in homeotropic alignment in the range of the SmC phase of the racemic compound *rac*-**1/12**. These domains 95 can be identified by slight rotation of the analyzer either clockwise or anti-clockwise out of the precise 90° orientation, which reverses the brightness of these domains (Fig. 4a-c).[9,11,13] Rotating the sample between the polarizers does not lead to such a change of brightness, thus excluding tilt director alignment as 100 the origin of this effect (Fig. S6†). In addition, though domains can also be recognized in the homeotropic SmC* phase of (*S*)-**1/12**, in this case there is no visible effect of the orientation of the polarizer (Fig. 4d-f). As there is no polar order in the SmC phase the origin of chirality must be due to the segregation of chiral 105 molecular conformers,[13] which is additionally supported by surface interaction.†† This indicates a strong chirality of the molecular conformations and a strong coupling between them. The cybotactic nature of the nematic phase and the absence of clear transition enthalpies at the phase transitions indicate a 110 nearly continuous growth of the coherence length of the smectic clusters throughout the N$_{cybA}$-SmA-SmC transitions with correlation lengths of ~67 nm at 105 °C, ~100 nm at 100 °C, ~110 nm at 90 °C and ~120 nm at 70 °C (Fig. 3d, Table S1). This indicates that already in the nematic phase the cybotactic 115 clusters are relatively large and increase continues in the smectic phases. Thus, in the SmA and SmC phases there is a remaining layer distortion providing soft layers which can be easily deformed into a TGB-like superstructure (Fig. 1). Therefore, the

weak helical twisting power of the (*S*)-2-methylbutyl group can provide a sufficiently strong chirality effect that TGB states are formed at the N*-SmA transition. These can be further stabilized over broader temperature ranges by planar surface anchoring. Only at lower temperature (< 70 °C), in the SmC phase region, the layer scattering becomes nearly resolution limited, indicating the development of almost non-distorted layers which inhibit TGB-like deformation (Fig. 3d).
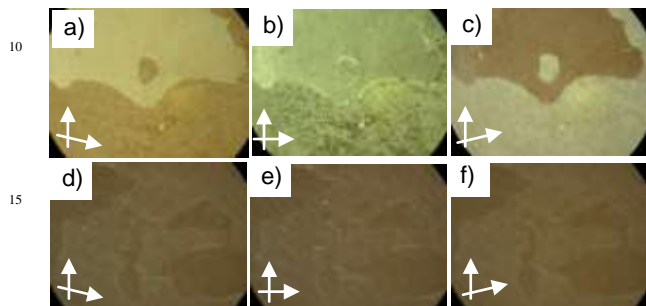


**Figure 4** Textures of the homeotropic SmC phases (a-c) of *rac*-**1/12** and (d-f) of (*S*)-**1/12** at *T* = 75 °C as observed (b,e) between crossed polarizers and between uncrossed polarizers with the analyzer rotated by 5° (a,d) clockwise or (c,f) counter-clockwise; reversal of brightness in the series (a-c) indicates chiral domains with opposite handedness, whereas there is no effect in the series (d-f) (see also Fig. S6†).

In summary, first observation of TGB structures in mesophases of bent-core mesogens is reported.‡‡ These are formed by molecules with a (*S*)-2-methylbutoxy stereogenic centre, known to have only weak helical twisting power. However, strong chirality of the molecular conformers, an imperfect layer structure and surface anchoring can stabilize the TGB states over broad temperature regions. These TGB-structures could probably be considered as intermediate steps at the transition from flat layers of smectic phases to the highly distorted optically isotropic dark conglomerate (DC) phases of some achiral BC mesogens[9,10] if conformational chirality effects become stronger and the layers become more frustrated by the layer-destabilizing effects of growing interface curvature and evolving polarization splay.§§

## Notes and references

*a Institute of Chemistry, Organic Chemistry, Martin-Luther University Halle-Wittenberg, Kurt-Mothes Str. 2, 06120 Halle, Germany. E-mail: carsten.tschierske@chemie.uni-halle.de; Fax: +49 345 5527346.*
*b Department of Chemistry, Yildiz Technical University, Davutpasa Yerlesim Birimi, TR-34220, Esenler, Istanbul, Turkey. E-mail ocak_hale@hotmail.com; Fax:+90 212 3834134.*

† Electronic Supplementary Information (ESI) available: [Synthesis, analytical data, DSC traces, additional XRD patterns, textures and other data]. See DOI: 10.1039/b000000x/

‡ The helical twisting power is an empiric measure of the effect of chirality on LC superstructures. It depends on molecular structural parameters, conditions (e.g. *T*), enantiomeric purity and type of superstructure. It is inversional proportional to the helical pitch and depends on the helicity of the molecular conformations, the energy barriers between enantiomorphic conformers and the degree of coupling of the stereogenic unit with the molecular conformational helicity.[5]

§ The birefringence in the homeotropic SmC* phases is much lower than in the SmC phase of *rac*-**12** (see Fig. 4), indicating the presence of a helix along the layer normal being larger than the wave length of light.

¶ That no switching peak could be observed even in the SmC* phases could be due to the known weak effect of the (*S*)-2-methylbutyl group on polar order, leading to very small values of spontaneous polarization.[5,14b] Also optically, no switching can be observed; this confirms that there is no switching or it takes place by rotation around the molecular long axis.

†† This kind of chiral SmC phase was previously reported for 4-cyanoresorcinol based BC molecules with azobenzene wings, and a local $SmC_sP_F$ structure was assumed to be responsible for chirality.[18] However the recent observation of chiral segregation in isotropic liquids[13] supports the possibility of spontaneous chiral segregation in SmC phases with a dense packing of the aromatic cores. This chiral segregation provides a helical distortion of the layers, thus giving rise to layer distortion and leading to amplification of small chirality effects.

‡‡ TGB-like twist states and TGB phases were observed for mixtures of chiral rod-like molecules with achiral bent-core molecules[19] or hockey-stick compound[20] and for chiral dimesogens with odd spacers.[17]

§§ A TGB-like structure has indeed been discussed as a possible organization in the DC phases,[21a] but only recently a DC-like random grain boundary phase of achiral hockey-stick LC was reported.[21 b]

1 D. B. Amabilino, *Chirality at the Nanoscale* (Wiley-VCH, Weinheim, 2009)
2 *Handbook of Liquid Crystals*, 2nd. Ed. (J. W. Goodby, P. J. Collings, T. Kato, C. Tschierske, H. F. Gleeson, P. Raynes,) Eds.), 2014, Wiley-VCH, Weinheim
3 C. Tschierske, *Angew. Chem. Int. Ed.*, **2013**, *52*, 8828-8878.
4 I. Dierking, *Symmetry* **2014**, *6*, 444-472
5 H-S. Kietzerow, C. Bahr (Eds), *Chirality in liquid crystals*, Springer, New York. NY, 2001
6 a) J. W. Goodby, M. A. Waugh, S. M. Stein, E. Chin, R. Pindak and J. S. Patel, *Nature*, **1989**, *337*, 449-452; b) J. W. Goodby *Curr. Opin. Coll. Interf. Sci.* 2002, 7, 326-332; c) M. Brunet, L. Navailles, and N. A. Clark, *Eur Phys. J. E*, 2002, 7, 5-11.
7 S. R. Renn and T. C. Lubensky, *Phys. Rev. A*, **1988**, *38*, 2132-2147.
8 H. T. Nguyen, M. Ismaili, N. Isaert, M. F. Achard; *J. Mater. Chem.* **2004**, *14*, 1560-1566.
9 a) R. A. Reddy and C. Tschierske, *J. Mater. Chem.*, **2006**, *16*, 907-961; b) Takezoe and Y. Takanishi, *Jpn. J. Appl. Phys.*, **2006**, *45*, 597-625; c) A. Eremin and A. Jakli, *Soft Matter*, **2013**, *9*, 615.
10 L. E. Hough, M. Spannuth, M. Nakata, D. A. Coleman, C. D. Jones, G. Dantlgraber, C. Tschierske, J. Watanabe, E. Körblova, D. M. Walba, J. E. Maclennan, M. A. Glaser, N. A. Clark, *Science* **2009**, *325*, 452.
11 H. Takezoe *Top. Curr. Chem.* **318**, 2012, 303-330.
12 V. P. Panov, R. Balachandran, J. K. Vij, M. G. Tamba, A. Kohlmeier, and G. H. Mehl, *Appl. Phys. Lett.* **2012**, *101*, 234106.
13 C. Dressel, T. Reppe, M. Prehm, M. Brautzsch, C. Tschierske, *Nat. Chem.* **2014**, *6*, 971-977.
14 a) H.-C. Jeong, S. Aya, S. Kang, F. Araoka, K. Ishikawa and H. Takezoe, *Liq. Cryst.*, **2013**, 40, 951–958; b) H. Ocak, B. Bilgin-Eran, M. Prehm, S. Schymura, J. P. F. Lagerwall and C. Tschierske, *Soft Matter*, **2011**, *7*, 8266–8280.
15 a) L. Kovalenko, M. W. Schröder, R. A. Reddy, S. Diele, G. Pelzl and W. Weissflog, *Liq. Cryst.* **2005**, *32*, 857–865; b) C. Keith, A. Lehmann, U. Baumeister, M. Prehm and C. Tschierske, *Soft Matter*, **2010**, *6*, 1704–1721.
16 I. Dierking, S. T. Lagerwall, *Liq. Cryst.* **1999**, 26, 83-95.
17 C. V, Yelamaggad, A. S. Achalkumar, N. L. Bonde, A. K. Prajapati, *Chem. Mater.* **2006**, *18*, 1076-1078.
18 M. Alaasar, M. Prehm, M. Nagaraj, J. K. Vij, C. Tschierske, *Adv. Mater.* **2013**, *25*, 2186-2191.
19 P Archer and I. Dierking, *Liq. Cryst.* **2006**, *33*, 257–265
20 V. Novotna, M. Glogarova, V. Kozmik, J. Svoboda, V. Hamplova, M. Kaspar and D. Pociecha, *Soft Matter*, **2013**, *9*, 647–653.
21 a) S. K. Lee, L. Shi, M. Tokita and J. Watanabe, *J. Phys. Chem. B,* **2008**, *112,* 6762–6766; b) D. Chen, H. Wang, M. Li, M. A. Glaser, J. E. Maclennana and N. A. Clark, *Soft Matter*, **2014**, *10*, 9105-9109.